

Surface plasmon assisted contact scheme nanoscale photolithography using an UV lamp

Dongbing Shao and Shaochen Chen^{a)}

Mechanical Engineering Department and Microelectronics Research Center, The University of Texas at Austin, Austin, Texas 78712

(Received 4 June 2007; accepted 20 December 2007; published 23 January 2008)

In this article, we present our study on surface plasmon (SP) assisted contact scheme nanoscale photolithography technique. Sub-100-nm features on a metallic mask, fabricated by e-beam lithography, were successfully transferred to a resist pattern in a setup close to traditional photolithography. Our previous work based on finite difference time domain simulation reveals the mechanism of SP-light coupling in the transferring and confining of light in surface plasmon assisted nanolithography (SPAN), which was demonstrated using 355 nm laser light. In this article, we extended our SPAN work to the use of UV light from a mercury lamp, which emits broadband, unpolarized, and incoherent light. Our experimental results show that sub-100-nm features can still be easily transferred using SPAN despite the light source used, proving SPAN to be an alternative nanopatterning technique that is simple, quick, and inexpensive. The experiments also showed interesting SP interference effects at the boundary of the mask. © 2008 American Vacuum Society. [DOI: 10.1116/1.2834688]

I. INTRODUCTION

The rapid advancements in nanotechnology demand convenient nanoscale patterning methods. Different techniques, such as electron-beam lithography,¹ imprint lithography,² scanning probe lithography,³ and dip-pen lithography,⁴ have been developed for this purpose. On the other hand, resolution enhancement techniques to overcome the diffraction limit in optical lithography are also attractive due to their high throughput and simplicity. Industry has been pursuing shorter wavelength light sources and immersion techniques; however, these lithography systems are getting more and more complex and expensive. Recently, there have been significant research interests in contact mode nanoscale photolithography. These research efforts take advantage of the sub-wavelength scale optical near-field phenomena that carry the high resolution image information, which is absent in the far field due to either cutoff by the optical system and/or intensity decay.

Contrary to the periodic treatment in solid state physics, the free electrons of a metal can be regarded as an electron liquid (plasma) of high density (about 10^{23} cm⁻³). While the electron density fluctuation may propagate through the bulk of a metal, another interesting wave phenomenon, which can be predicted by Maxwell's equations, happens at the interface of a metal and a dielectric material. The electrons on a metal surface can exhibit coherent fluctuations caused by, for example, an incident electromagnetic (EM) wave. Because of the existence of the boundary, net charges are accumulated at the surface, which produces another local EM field in the dielectric side of the interface. Such an interaction between the surface charges and the EM field constitutes the surface plasmons (SPs), which propagate along the interface. The

field, perpendicular to the surface, decays exponentially as it moves away from the surface, which is known as evanescent or near field in nature. In other words, the EM energy of SPs is trapped at the surface and does not radiate.

Analytically solving Maxwell's equations under appropriate boundary conditions reveals that such phenomena have to be in the TM-mode polarization for two-dimensional conditions. However, the surface mode wave vector is always greater than that of the photon in the dielectric medium; thus SPs cannot be directly excited by light due to their momentum mismatch. Additional momentum has to be provided to bridge the gap. Ebbesen *et al.* found that periodic perforations in a metal film can actually serve such a purpose and result in surprisingly high optical transmission⁵ and have triggered tremendous interest in understanding the mechanism behind the enhanced transmission and SP-light coupling.⁶⁻¹²

There has been pioneering work combining high transmission phenomena with contact mode photolithography to overcome the diffraction limit. Srituravanich *et al.*¹³ demonstrated plasmonic nanolithography by utilizing SPs transmitted through an array of subwavelength two-dimensional holes on an aluminum film, which is believed to most strongly support SPs at UV wavelengths. To show this concept, a negative tone photoresist (SU-8) was directly spun on a plasmonic mask. A sub-100-nm dot array pattern on a 170 nm period was successfully obtained using an exposure radiation of 365 nm wavelength. Luo and Ishihara¹⁴ experimentally demonstrated a sub-100-nm linewidth photolithography by utilizing surface plasmon polaritonic interference, in the optical near field, excited by a wavelength of 436 nm. Surface plasmon polariton results in a strongly enhanced nanoscale spatial distribution and exposes the thin layer of photoresist directly below the mask. The features on the mask have a periodicity of 300 nm, and the opening is 1/5

^{a)}Electronic mail: shaochen.chen@engr.utexas.edu

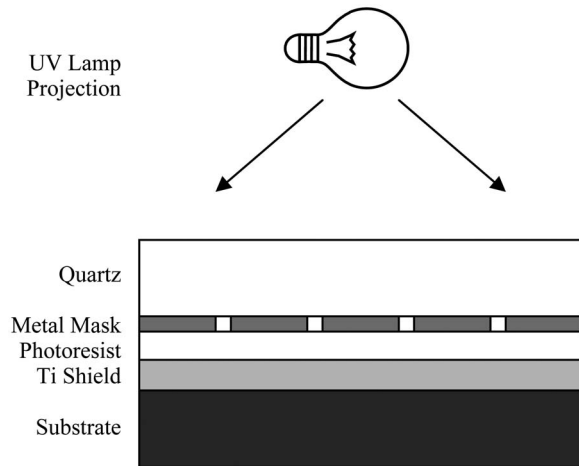


FIG. 1. Schematic view of the surface plasmon assisted lithography scheme.

of the periodicity. The features on the photoresist have a periodicity of 100 nm and the linewidth is about 50 nm. The light transmitted is not only found at the locations below the aperture but also below the metal surfaces. Since the illuminating source consists of the light directly emitted from the aperture and the optical near field produced by SP interference, the pattern produced in this approach is not one-to-one matched with the mask pattern.

In photolithography, it is desirable to have arbitrary nanoscale patterning capabilities while the system setup remains as simple as possible. In order to satisfy this objective, the two fundamental issues of light at subwavelength scales, transmission and diffraction, have to be resolved to a certain degree. The discovery of enhanced transmission through perforated metal films and the understanding of the mechanism behind this phenomenon have paved the way in overcoming the transmission issue by utilizing SP-light coupling. We have demonstrated a nanolithography scheme utilizing SP-light coupling, coined surface plasmon-assisted nanolithography (SPAN), to overcome the two issues.¹⁵ The mechanism is understood with the help of finite difference time domain (FDTD) modeling: the surface plasmons excited on the mask enhance the light transmission through the subwavelength aperture, while the surface plasmons excited on the substrate help to confine the light intensity to the space behind the mask aperture by coupling to the incident light. In this article, UV light from a mercury lamp is used instead of 355 nm laser light to expose a thin layer of SU-8, a negative tone photoresist. We also discuss the proximity effects due to surface plasmon interference, which are unique phenomena in SPAN.

II. EXPERIMENTAL SETUP

The schematic representation of the setup is shown in Fig. 1. In this study, we used a commercial UV aligner (HTG, 365 nm) to expose an 80 nm thick photoresist spin coated on an 80 nm Ti film on a silicon substrate. The ultraviolet light from the mercury lamp has a spectrum with several peaks

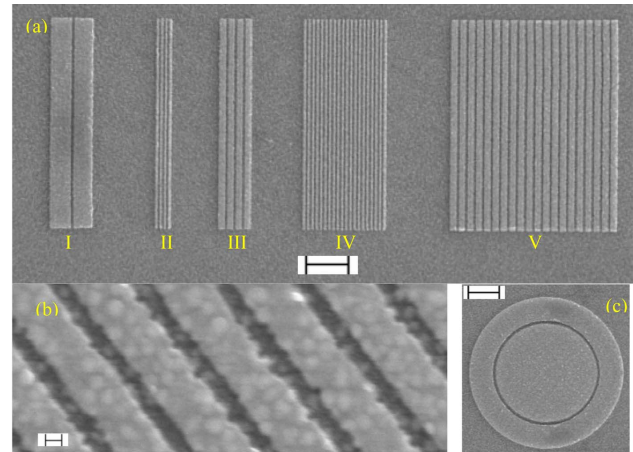


FIG. 2. Scanning electron microscopy (SEM) pictures of a Ti mask used for SPAN with UV light. (a) Overview of grating structures used for SPAN, scale bar=2 μm . (b) Close view of a grating structure with 80 nm aperture and 400 nm period, scale bar=100 nm. (c) Close view of a ring aperture, scale bar=2 μm .

and the maximum peak is centered at 365 nm with a full width at half maximum of about 20 nm. Although the optical properties of metals, for example, titanium, do not vary significantly across the UV range, the optical properties of silicon change dramatically.¹⁶ Since the optical penetration depth of UV light in titanium is only about 30 nm, we believe that by using a titanium shield layer of approximately 60 nm, the variation of optical properties of silicon across the UV emission spectrum should not be an issue anymore.

The nanolithography mask was fabricated by first patterning lines of e-beam resist (ZEP520) on a quartz substrate using an advanced electron beam lithography machine. The quartz mask we used has a layer of indium tin oxide (ITO) of about 100 nm thickness to facilitate the e-beam writing of polymethyl methacrylate on the quartz substrate. The ITO layer accounts for the roughness of the final mask. The mask was then patterned by depositing 70 nm titanium using electron-beam evaporation and lift-off. The mask patterns consist of both grating structures and a ring aperture as shown in Fig. 2. The gratings have an aperture width of 80 nm with different periodicities (200 or 400 nm) and number of apertures.

SU-8 (Microchem®), a negative near-UV photoresist (refractive index=1.67) was employed in the photolithography experiments and was spun on the Ti-coated silicon substrate to a thickness of 80 nm. During lithography, the mask and the sample were held in close contact by applying a pressure. The sample was then exposed in the UV aligner for 2 min and directly developed in SU-8 developer for 40 s and gently dried using an air gun.

The lithography results for the grating mask vary depending on both the number of apertures and periodicity. For grating mask patterns that have a period of 200 nm, the lithography resulted in almost no contrast (patterns II and IV in Fig. 3). In this case, the FDTD modeling has predicted satisfying contrast, although the periodicity is almost at the minimum limit. Considering the mask defects, which is ex-

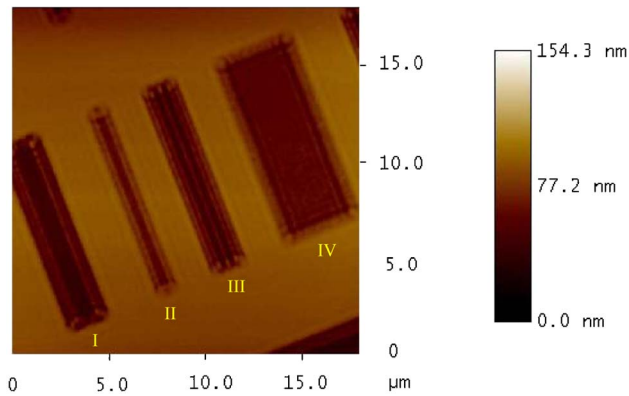


FIG. 3. AFM characterization of patterns transferred to SU-8 using the grating mask patterns I, II, III, and IV in Fig. 2(a).

plained early and shown in Fig. 2(b), this result is not very surprising. The pattern of gratings that have a period of 400 nm was transferred fairly well for a different number of apertures, as seen in both Fig. 3 (pattern III) and Fig. 4. From Fig. 4, the atomic force microscopy (AFM) results show that the pattern in the resist has a height of about 35 nm, which is believed to be partially due to the shrinkage of SU-8 during development.

The pattern of a single aperture was not transferred to the resist, as seen in Fig. 3 (pattern 1 from the left). This is somewhat of an interesting surprise. According to our FDTD modeling, the detail of which is explained elsewhere,¹⁷ both the single aperture and aperture arrays have good light confinement, with a slight difference in contrast. There might be two reasons to explain this unexpected result. First, in both modeling and experiment, the termination of the metal mask at the ends, on each side of the single aperture, may physically place an actual period for the pattern in both modeling and the physical mask. These two pitches could easily be different without notice, which results in the discrepancy. Second, although the single aperture may be able to confine the light as in the case of the aperture array, it may not be efficient in collecting the light impinging on it, thus requiring more exposure time. Also, in simulation, defects in the mask apertures were not accounted for.

The boundary effect can be seen for all the grating patterns mentioned. This effect seems similar to the proximity effect in e-beam lithography and photolithography, which is already understood and can be corrected by certain design correction rules. However, interestingly enough, in our case, the lithography results at the boundary are enhanced rather than weakened as in the optical/e-beam proximity effect. Ap-

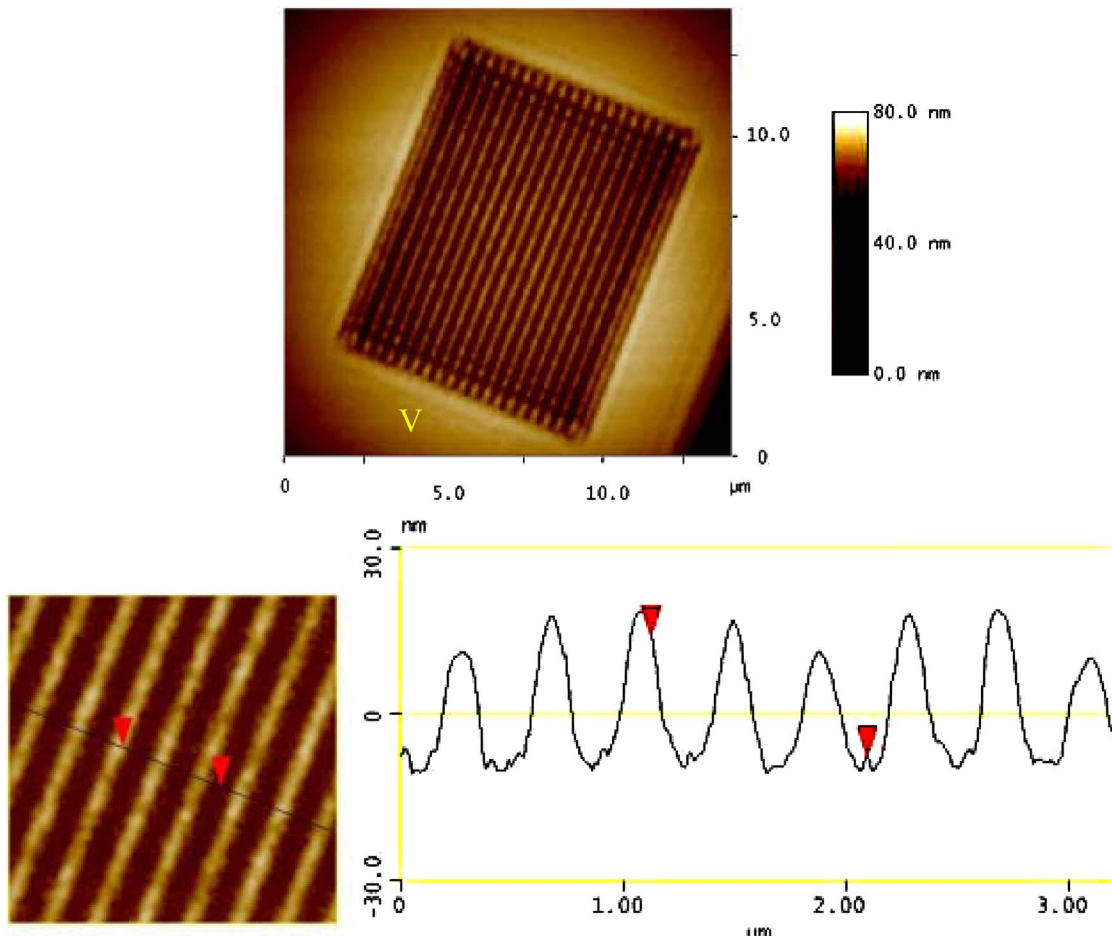


FIG. 4. Lithography results with grating mask pattern V in Fig. 2(a) (periodicity=400 nm).

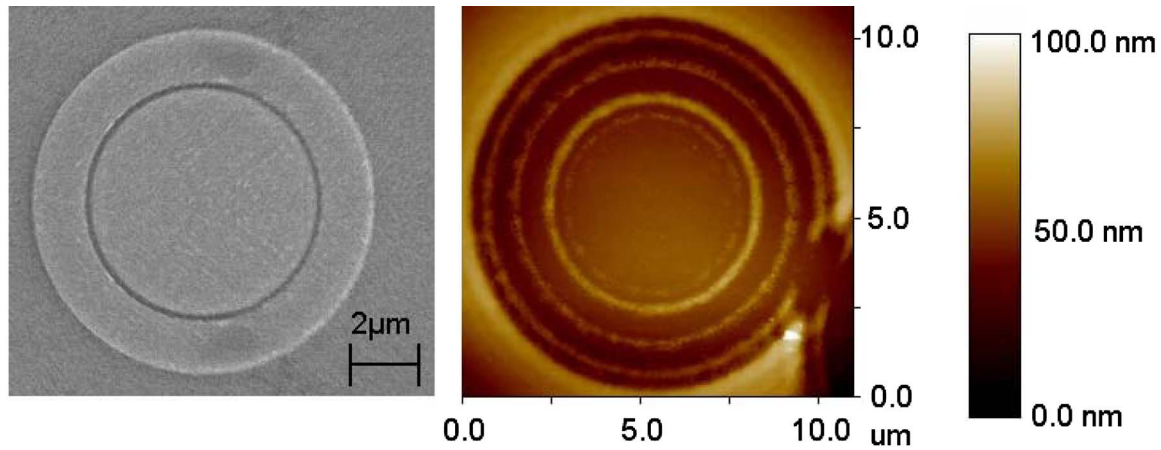


FIG. 5. (a) A SEM image of the ring aperture, scale bar=2 μm . (b) AFM characterization of lithography results with the ring aperture.

parently, such an effect is related to the propagation and interference of SPs on the metal film surface. Further investigation in this can help us to better understand the mechanism of surface plasmons in SPAN and to create design rules to minimize the boundary effect.

The SPAN result for a ring aperture is shown in Fig. 5. In this case, obvious SP interference can be observed. The mask ring pattern has an outer diameter of 10 μm and a ring aperture of 6.5 μm in diameter. The pattern in the resist has an outer diameter of 10 μm ; however, not only are there several ring structures produced in the photoresist, the primary ring has a diameter slightly different from that of the ring aperture in the mask. Again, this can be explained by the interference of propagating SPs.

III. DISCUSSION

The experimental results match fairly well with our simulation using FDTD. However, our lithography is done using UV light from a mercury lamp, while in the FDTD simulation the light source is assumed to be monochromatic, polarized, and coherent. The discrepancies can be explained by the following reasons. First, the optical properties (the refractive index and extinction coefficient) of the materials (aluminum, SU-8, and quartz) used in SPAN do not vary significantly in the UV range;¹⁶ thus, the use of a multichromatic light source does not significantly alter the EM field distribution and the structure produced by SPAN. Second, the unpolarized light source can be thought of as the superposition of its TM and TE components. It was found that the transmission through subwavelength metallic apertures in the TE mode is prohibited due to the absence of SP involvement;⁵ thus, the contribution from the TE mode component of UV light is either trivial or overshadowed by the TM mode counterpart.

As discussed previously, the Ti shield layer is crucial in SPAN using UV light. It helps to focus the light intensity in the photoresist to achieve high density nanoscale patterning. Also, the 80 nm thick titanium shield is thick enough to absorb the light as it reaches the substrate since the penetration depth of titanium at 355 nm wavelength is about 30 nm.

Thus, the optical properties of the substrate are not important to the lithography results and virtually any substrates can be used. Once the patterns form in the photoresist, the titanium shield layer can be patterned and used as a metal mask to pattern the underlying substrate.

So far, the minimum linewidth demonstrated in our experiments is still only about 100 nm. Even if the lines could be smaller, say 80 nm, the roughness of the line, which is the result from the roughness of the mask pattern, makes it difficult to characterize the difference. Despite the defects in the SPAN mask, our results are encouraging and we believe that there is still room to improve the SPAN process in terms of minimum linewidth. The feature size in SPAN could be further scaled down, limited theoretically by the validity of the dielectric function of the material, and practically by the fabrication of the mask. The former limit indicates that it can reach a dimension on the order of 20 nm; however, that would place a very critical requirement on mask fabrication. By improving SPAN mask quality, for example, by planarization of the mask substrate, we believe the lithography results can be significantly improved.

IV. SUMMARY

In this article, we investigated subwavelength light confinement by utilizing SP-light coupling and our results demonstrate that photolithography resolution can be extended to subwavelength scales by simultaneously exciting surface plasmons on the metallic mask and the substrate. Without any additional equipment or added complexity to mask design, one-to-one pattern transfer has been achieved. UV light from a mercury lamp was used as the light source to photo-initiate an 80 nm thick photoresist on a silicon substrate coated with a titanium layer of 80 nm thickness. Simulation results by the finite difference time domain method have predicted the results and also revealed the contribution of surface plasmons excited on both the metallic mask and the Ti shield in helping to spatially confine the light. Our lithography scheme is a convenient, inexpensive, high-throughput nanofabrication method. The feature size using our method

could be further scaled down, limited theoretically by the validity of the dielectric function of the material, and experimentally by the fabrication of the mask.

ACKNOWLEDGMENTS

This work was performed in part at the Microelectronics Research Center at UT-Austin of National Nanofabrication Infrastructure Network supported by National Science Foundation under award No. 0335765. Financial support by research grants (CMMI 0609345 and CMMI 0600104) from the National Science Foundation is greatly appreciated. The authors appreciate the computer support from the Intel's Higher Education Program. The authors would like to thank Li Wang for help of e-beam lithography and David Fozdar's help with this article.

¹C. Vieu *et al.*, *Appl. Surf. Sci.* **164**, 111 (2000).

²S. Y. Chou, P. R. Krauss, and P. J. Renstrom, *Science* **272**, 85 (1996).

³F. H'dhili, R. Bachelot, G. Lerondel, D. Barchiesi, and P. Royer, *Appl. Phys. Lett.* **79**, 4019 (2001).

⁴R. D. Piner, J. Zhu, F. Xu, S. Hong, and Chad A. Mirkin, *Science* **283**, 661 (1999).

⁵T. W. Ebbesen, H. J. Lezec, H. F. Ghaemi, T. Thio, and P. A. Wolff, *Nature (London)* **391**, 667 (1998).

⁶H. Raether, *Surface Plasmons on Smooth and Rough Surfaces and on Gratings*, Springer Tracts in Modern Physics Vol. 111 (Springer, Berlin, 1988).

⁷J. Pendry, *Science* **285**, 1687 (1999).

⁸H. F. Ghaemi, T. Thio, D. E. Grupp, T. W. Ebbesen, and H. J. Lezec, *Phys. Rev. B* **58**, 6779 (1998).

⁹E. Popov, M. Nevriere, S. Enoch, and R. Reinisch, *Phys. Rev. B* **62**, 16100 (2000).

¹⁰L. Martin-Moreno *et al.*, *Phys. Rev. Lett.* **86**, 1114 (2001).

¹¹S. Collin, F. Pardo, R. Teissier, and J. L. Pelouard, *Phys. Rev. B* **63**, 033107 (2001).

¹²W. L. Barnes, W. A. Murray, J. Dintinger, E. Devaux, and T. W. Ebbesen, *Phys. Rev. Lett.* **92**, 107401 (2004).

¹³W. Srituravanich, N. Fang, C. Sun, Q. Luo, and X. Zhang, *Nano Lett.* **4**, 1085 (2004).

¹⁴X. G. Luo and T. Ishihara, *Appl. Phys. Lett.* **84**, 4780 (2004).

¹⁵D. B. Shao and S. C. Chen, *Appl. Phys. Lett.* **86**, 253107 (2005).

¹⁶E. D. Palik, *Handbook of Optical Constants of Solids*, Academic Press Handbook Series (Academic, Orlando, 1985).

¹⁷D. B. Shao and S. C. Chen, *Opt. Express* **13**, 6964 (2005).